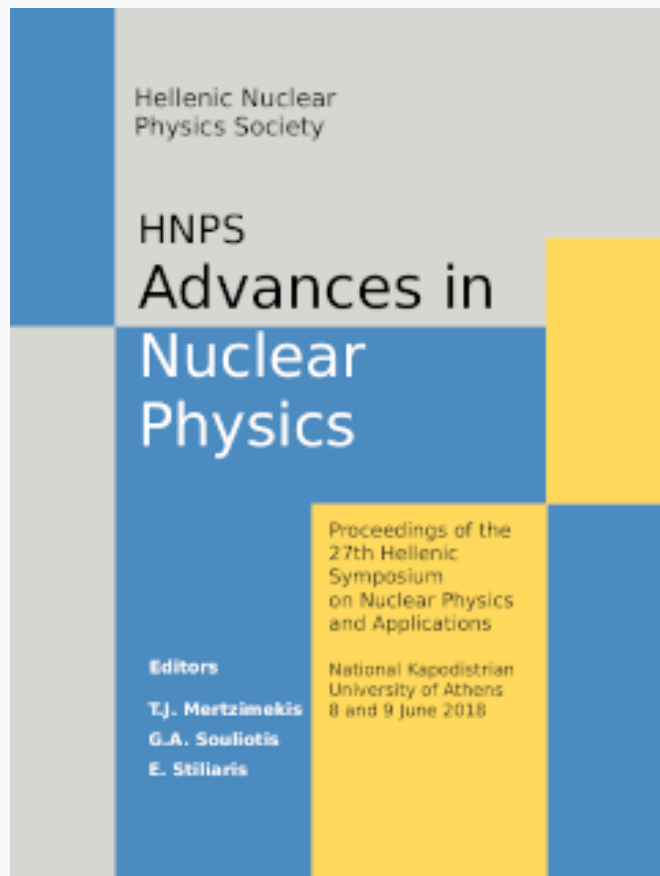


HNPS Advances in Nuclear Physics

Vol 26 (2018)

HNPS2018



First results of the differential cross sections of ${}^9\text{Be}(\text{d},\text{d}0)$ at energies and angles suitable for Elastic Backscattering Spectroscopy

E. Ntemou, M. Kokkoris, A. Lagoyannis, C. Lungu, K. Mergia, K. Prekete-Sigalas, P. Tsavalas

doi: [10.12681/hnps.1812](https://doi.org/10.12681/hnps.1812)

To cite this article:

Ntemou, E., Kokkoris, M., Lagoyannis, A., Lungu, C., Mergia, K., Prekete-Sigalas, K., & Tsavalas, P. (2019). First results of the differential cross sections of ${}^9\text{Be}(\text{d},\text{d}0)$ at energies and angles suitable for Elastic Backscattering Spectroscopy. *HNPS Advances in Nuclear Physics*, 26, 158–165. <https://doi.org/10.12681/hnps.1812>

First results of the differential cross sections of ${}^9\text{Be}(\text{d},\text{d}_0)$ at energies and angles suitable for Elastic Backscattering Spectroscopy

E. Ntemou^{1,2,a}, M. Kokkoris¹, A. Lagoyannis², C. Lungu⁴, K. Mergia³, K. Prekete-Sigalas^{1,2}, P. Tsavalas³

¹*Department of Physics, National Technical University of Athens, Zografou campus, 15780 Athens, Greece*

²*Tandem Accelerator Laboratory, Institute of Nuclear Physics, N.C.S.R. “Demokritos”, Aghia Paraskevi, 15310 Athens, Greece*

³*Institute of Nuclear and Radiological Science and Technology, Energy and Safety, N.C.S.R. “Demokritos”, Aghia Paraskevi, 15310 Athens, Greece*

⁴*National Institute for Laser, Plasma and Radiation Physics, 077125 Magurele, Bucharest, Romania*

Abstract The differential cross sections of the ${}^9\text{Be}(\text{d},\text{d}_0)$ elastic scattering were determined in the present work in the energy range of $E_{\text{d,lab}} = 740 - 2200$ keV in variable steps, mainly 20 keV at five backscattering angles (120° , 140° , 150° , 160° and 170°). The measurements were performed at the 5.5 MV TN11 HV Tandem Accelerator of the N.C.S.R. “Demokritos” implementing a high precision goniometer. The target used was a thin Si_3N_4 target with a Beryllium layer on top. The obtained differential cross section values are compared to the ones existing in literature and the observed similarities and discrepancies are discussed.

Keywords EBS; Beryllium; Differential cross section; Elastic scattering

INTRODUCTION

Although beryllium (100% ${}^9\text{Be}$, with traces of ${}^7\text{Be}$ and ${}^{10}\text{Be}$) is a relatively rare element in the universe, it has numerous applications in the industry. It is added as an alloying element to copper (beryllium copper), aluminum, nickel and iron as it improves many physical properties. It is commonly used in mechanical and defense applications, namely as aerospace material for aircraft components, guided missiles, satellites and space crafts due to its high metal flexural rigidity, thermal stability, thermal conductivity and low density. Moreover, it constitutes the most crucial material in plasma-facing components as it has the ability to getter or bury oxygen in the absence of chemical reactivity with hydrogen, and because of its reasonably high melting point and low-Z. Thus, a great need emerges for the accurate quantitative determination of beryllium depth profiling, especially for the assessment of beryllium deposition and erosion processes which go hand in hand with the safety of tokamak, by analyzing samples from fusion devices, via the implementation of all Ion Beam Analysis (IBA) techniques.

^a Corresponding author, e-mail: ntemou@inp.demokritos.gr

A versatile technique for the depth profiling of light elements and the accurate quantitative determination of elemental concentrations of complex matrices consisting of several low- and medium- Z elements is the d- Elastic Backscattering Spectroscopy (EBS). However, the most important drawback in the implementation of the d-EBS technique for the beryllium case is the fact that only scarce data exist in the literature with many discrepancies among them.

The present work aims at contributing in this field, by studying the deuteron elastic scattering on ${}^9\text{Be}$, in the energy range $E_{d,\text{lab}}=740\text{-}2200\text{ keV}$, in steps of $\sim 20\text{ keV}$ and for laboratory scattering angles of 120° , 140° , 150° , 160° and 170° . The experiment was carried out at the 5.5 MV Tandem Accelerator at NCSR “Demokritos” and the target used was a thin Si_3N_4 self-supporting foil produced by Silson Ltd., with a thin beryllium layer placed on top by means of reactive magnetron sputtering. The detection system consisted of five, $500\text{ }\mu\text{m}$ thick, silicon surface barrier (SSB) detectors, mounted on a high precision goniometer inside a cylindrical chamber ($R\sim 40\text{ cm}$). The obtained differential cross-section datasets are compared to the already existing ones in literature and an attempt is made to explain the occurring similarities and differences. The datasets from the present work after the finalization of the analysis will become available to the scientific community via IBANDL (<https://www-nds.iaea.org/exfor/ibandl.htm>, Ion Beam Analysis Nuclear Data Library).

EXPERIMENTAL SETUP

The experiment was carried out at the 5.5 MV Tandem accelerator laboratory of the N.C.S.R. “Demokritos”, Athens, Greece and the deuterons were accelerated to energies $E_{d,\text{lab}}=0.74\text{-}2.2\text{ MeV}$ in steps of 20 keV and led to a cylindrical goniometer of $R\sim 40\text{cm}$. For the charge measurements (charge collection and current integration) a long faraday cup was implemented at the scattering chamber ($L\sim 1.5\text{ m}$). The final beam energy was determined by nuclear magnetic resonance (NMR) measurements with a ripple of $1.15 \pm 0.60\text{ keV}$, as verified by the ${}^{99}\text{Al}(\text{p},\gamma){}^{28}\text{Si}$ reaction using a 18% HPGe detector. The detection system consisted of five Si surface barrier detectors with thicknesses of $\sim 500\text{ }\mu\text{m}$ along with the corresponding electronics.

The target used was an ultra-thin, high purity self-supporting Si_3N_4 membrane with a nominal thickness of 75 nm (Silson Ltd.). A thin beryllium layer was deposited on top by means of reactive magnetron sputtering. The target was placed perpendicularly to the beam axis and at a distance of $\sim 10\text{ cm}$ from the detectors. Orthogonal slits were placed in front of the detectors in order to reduce the angular uncertainty (to $\pm\sim 1^\circ$) while allowing for an adequate solid angle to be subtended by the detectors. Moreover, aluminum tubes with variable lengths and a diameter of $\sim 1\text{ cm}$ were placed in front of the detectors in order to impede scattered particles from the chamber and/or the faraday cup to contribute to the background of the obtained spectra. A typical spectrum is shown in Fig.1 (a) for the deuteron energy $E_{d,\text{lab}} = 1260\text{ keV}$ and the scattering angle $\theta = 160^\circ$, along with the corresponding peak identification.

DATA ANALYSIS, RESULTS AND DISCUSSION

The calculation of the differential cross-section values was accomplished using the relative measurement technique [1] and in particular with respect to the differential cross sections of the ${}^{nat}\text{Si}(\text{d},\text{d}_0){}^{nat}\text{Si}$ elastic scattering which does not deviate from the Rutherford formula at $E_{d,\text{lab}} = 1000$ keV for the same scattering angle [2]:

$$\left(\frac{d\sigma}{d\Omega}\right)_{E,\theta}^{{}^9\text{Be}} = \left(\frac{d\sigma}{d\Omega}\right)_{Ruth,\text{Si},\theta}^{1000} \times \frac{Y_{{}^9\text{Be}} \times Q_{Ruth}^{1000}}{Y_{\text{Si},Ruth}^{1000} \times Q_{Be}} \times \frac{N_t^{Si}}{N_t^{Be}}$$

In the equation above, E corresponds to the energy at the half of the target thickness, θ is the scattering angle, $\left(\frac{d\sigma}{d\Omega}\right)_{Ruth,\text{Si},\theta}^{1000}$ is the differential cross section for the scattering of deuterons on ${}^{nat}\text{Si}$ at the energy of $E_{d,\text{lab}} = 1000$ keV, $Y_{{}^9\text{Be}}$ corresponds to the integrated area of the peaks due to the deuteron elastic scattering on ${}^9\text{Be}$, $Y_{\text{Si},Ruth}^{1000}$ to the integrated area of the peak due to the deuteron elastic scattering on ${}^{nat}\text{Si}$ at $E_{d,\text{lab}} = 1000$ keV, Q to the number of impinging deuteron ions in each case, whereas N_t^{Si} , N_t^{Be} are the atomic areal densities of the ${}^{nat}\text{Si}$ at the Si_3N_4 layer and of the ${}^9\text{Be}$ respectively.

The term $\left(\frac{d\sigma}{d\Omega}\right)_{Ruth,\text{Si},\theta}^{1000}$ was calculated using Rutherford's formula along with a correction factor due to the screening effect over the whole studied energy range ($E_{d,\text{lab}} = 0.84$ - 2.2 MeV).

The experimental yields, $Y_{{}^9\text{Be}}$ and $Y_{{}^{nat}\text{Si}}$ were determined by integration/fitting of the experimental peaks after a background subtraction using the SPECTRW code [3]. However, at some energies and angles an overlap occurs between the ${}^9\text{Be}(\text{d},\text{d}_0)$ elastic scattering and the ${}^{12}\text{C}(\text{d},\text{p}_1)$ reaction peaks, as presented in Fig. 1 (b) for the deuteron energy $E_{d,\text{lab}} = 1320$ keV and for the scattering angle $\theta = 160^\circ$. This is not the first case that the inevitable presence of carbon in the target (due to the manufacturing process of the target and the carbon buildup accumulated during the experiment) overlaps with the peak under study and the followed procedure in this case was the same as in the elastic scattering of deuterons in Li-7 by Prektes-Sigalas et al. [4].

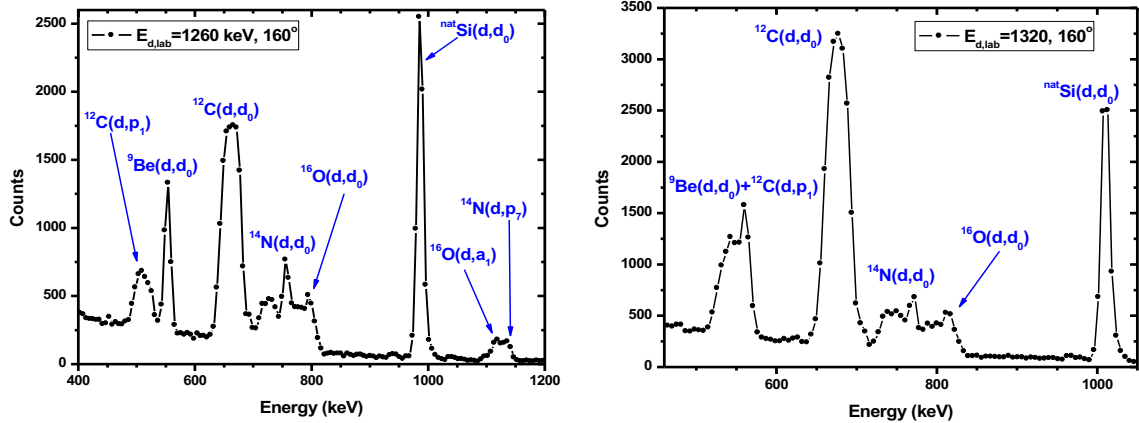


Fig. 1. (a) and (b) Experimental d-EBS spectrum at $E_{d,\text{lab}}=1260$ keV, $\theta=160^\circ$ and $E_{d,\text{lab}}=1320$ keV, $\theta=160^\circ$, respectively along with the corresponding peak identification

The Q_{Ruth}^{1000} and Q_{Be} were determined using the current integrator during the experiment with a systematic error of $\sim 6\%$.

The ratio N_{Au}/N_{Si} was calculated using two techniques; the p-EBS and the transmission ERDA one. The determination of the target thickness ratio with the p-EBS technique was accomplished using the SIMNRA code v.6.94 [5] and the proton spectra taken at energies $E_{p,lab} = 1200$ and 1500 keV, for this exact purpose under the same experimental setup. The simulation of the proton spectra was carried out using the same geometry, a very small energy step in the incoming and outgoing protons, the effect of multiple scattering, ZBL stopping power data along with the latest corrections for silicon [6,7] and Chu and Yang's straggling model as implemented in the SIMNRA code. The proton spectra were analyzed using the non-Rutherford evaluated data for proton elastic scattering on ^{12}C , ^{14}N , ^{16}O , ^{nat}Si , as obtained via the online calculator SigmaCalc 2.0 [<http://sigmacalc.iate.obninsk.ru/>]. For the simulation of the $^9Be(p,p_0)$ peak the dataset by Liu et al. taken at $\theta = 170^\circ$ [8] was used which was in agreement with the data by Krat et al. taken at $\theta = 165^\circ$ [9] within 4%. It should be noted here that the proton beam energies were selected far from existing minima and maxima of the $^9Be(p,p_0)$ elastic scattering in order to maximize accuracy. In more details, the procedure that was repeated for every proton beam was the following: The thickness of silicon was kept constant and the $Q \times \Omega$ product was slightly changed in order to achieve an agreement better than 1% in the integrated counts of the silicon peak between the simulated and the experimental spectrum. Subsequently, the thickness of the beryllium layer was determined for every proton beam energy. The average value of the N_{Si}/N_{Be} ratio was found equal to 0.20 ± 0.01 with a relative statistical error of 5%. However, systematic uncertainties, that are not included in the statistical error, may originate from the deviations between compiled and experimental stopping power data for protons impinging on silicon which can be found in SRIM (<http://www.srim.org/>) and can be as high as $\sim 8\text{-}9\%$. An example of an experimental proton spectrum along with the simulation results is shown in Fig. 2 for the proton energy $E_{p,lab} = 1500$ keV and the scattering angle $\theta = 170^\circ$, along with the corresponding peak identification. This graph reveals that the reproduction of the experimental spectrum is quite satisfactory. The second technique used for the target thickness determination was the transmission ERDA one with an oxygen beam at $E_0 = 11.75$ MeV and for the scattering angle of $\theta = 30^\circ$. The analysis of the obtained spectrum was accomplished using the SIMNRA and Rutherford cross section values for all the elements existing in the target, even for the case of oxygen ions from the beam scattered by oxygen ions in the target which normally follows the Mott scattering formula but there is no existing code simulating this process. The experimental spectrum along with the simulated one and the corresponding peak identification are presented in Fig. 3. The target thickness value for the ratio obtained by this technique was 0.221 with a systematic error $< 5\%$, originating from the deviation between stopping power compilations and theory. Consequently, the deviation between the two techniques was $< 10\%$. It should be noted here that a limiting factor in the reliability of the transmission ERDA technique exists in this particular case: The 'safe' beam energy (implying a 5 fm distance between the surfaces of the projectile and target nuclei) in order for the interaction of

the oxygen beam and the beryllium ions in the target to be purely Coulomb (i.e. beam energy well below the Coulomb barrier) is 10.424 MeV, meaning that the energy of the oxygen beam used in the present experiment slightly exceeds this constraint, thus some deviations of the Rutherford formula could in principle be expected.

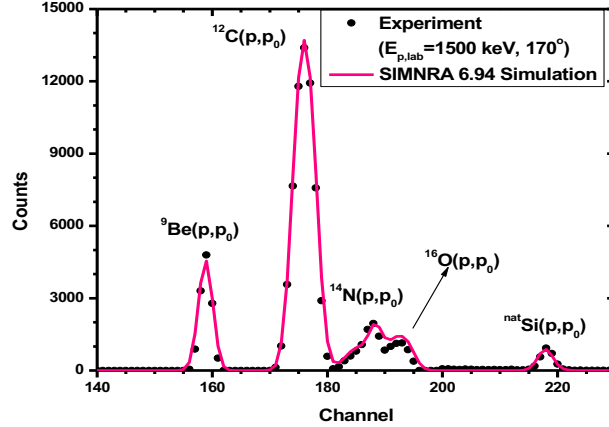


Fig. 2. Experimental and SIMNRA simulated, p-EBS spectrum at $E_{p,\text{lab}}=1500$ keV and the scattering angle of 170° , along with the corresponding peak identification.

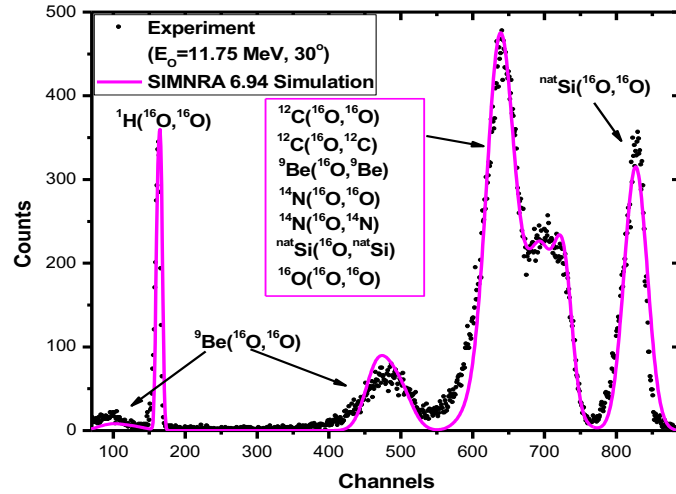
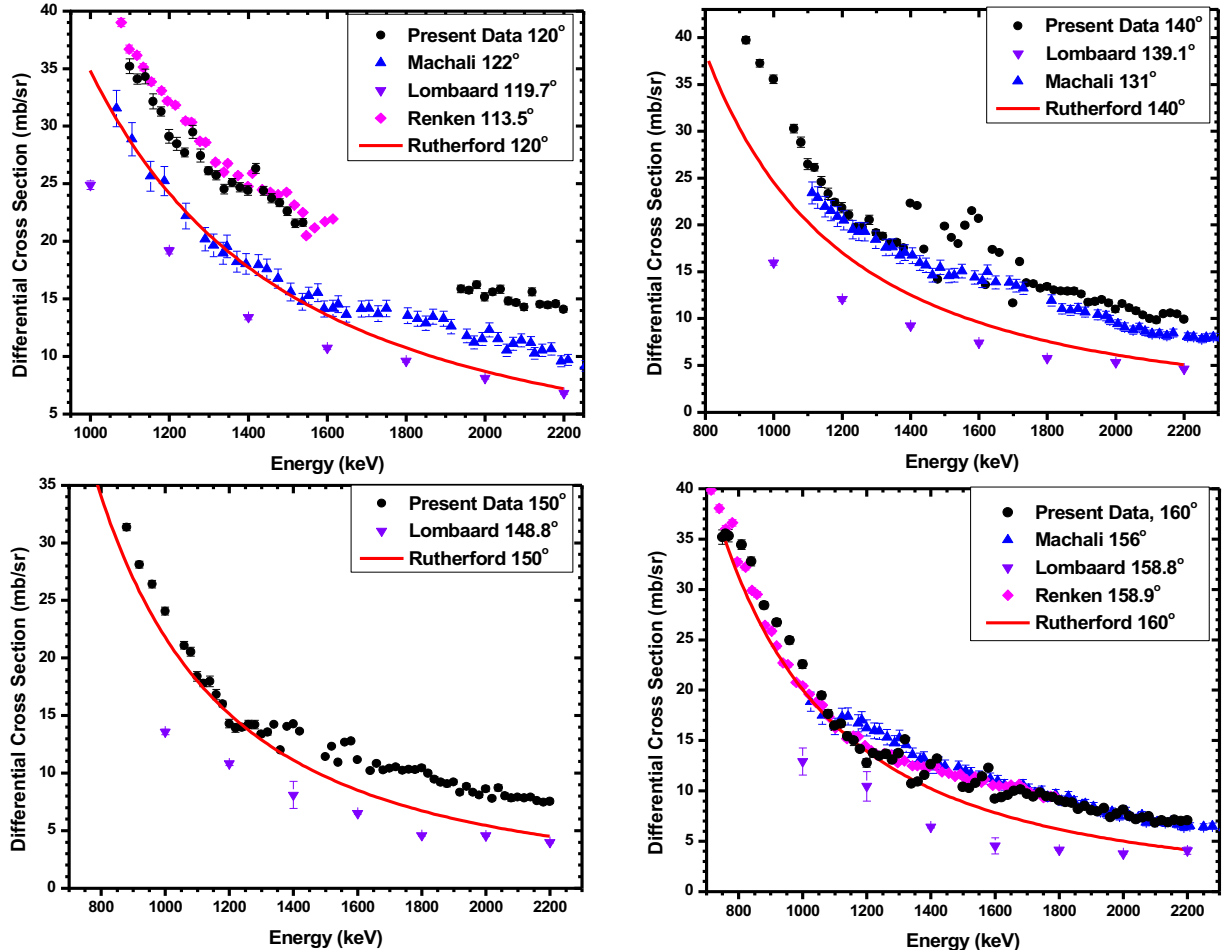


Fig. 3. Experimental and SIMNRA simulated, transmission ERDA spectrum at $E_{o,\text{lab}}=11.75$ MeV and the scattering angle of 30° , along with the corresponding peak identification.

The determined differential cross sections for the deuteron elastic scattering on beryllium for five scattering angles (120° , 140° , 150° , 160° , 170°) are presented in graphical form (Figs. 4a-e). The total statistical experimental uncertainty was calculated to be $\sim 8\text{-}15\%$ for the region where the $^{12}\text{C}(\text{d},\text{p}_1)$ parasitic contribution was present, whereas for all other cases it did not exceed $\sim 5\%$. The

systematic errors originating from the charge calculation ($\sim 6\%$) and the target thickness determination technique ($\sim 10\%$) are excluded from the calculation of the total statistical uncertainty budget. All existing datasets from literature according to the closest experimental scattering angle under study are also included in the graphs. For all three scattering angles in common (120° , 140° , 160°) with Machali et al. [10] there seems to be a good agreement except for the case of 120° , where the data obtained in the past seems to be systematically lower. Although there is no clear reason, large deviations are observed between the present data and the data by Lombaard et al. [11] over the whole energy range and for all scattering angles. Concerning the discrepancies with the data by Renken et al. [12], there seems to be a good agreement within errors for the case of 160° , whereas for 120° deviations are observed at lower energies. Furthermore, comparing the present datasets to the ones calculated using the Rutherford formula small deviations are present at low energies while at higher ones these deviations tend to increase, except for the angle of 140° where large deviations are observed over the whole energy range. The whole structure of the obtained cross-section values could be attributed to the overlapping levels of the compound nucleus $^{11}\text{B}^*$ with energies 16432 keV ($\Gamma = < 30$ keV), 17310 keV ($\Gamma \sim 1$ MeV), 17500 keV ($\Gamma = 116$ keV) and 18000 keV ($\Gamma = 870$ keV). The latter level is above the energy range studied in the present work but it affects the cross-section values due to its large amplitude. Finally, it should be noted here that a rather strange behavior is observed in the energy range where the contribution of the $^{12}\text{C}(\text{d},\text{p}_1)$ reaction was subtracted (except for the case of 120° where no available datasets exist in literature) and a more thorough re-evaluation of the analysis must be done, otherwise the data from this energy range must be excluded from the final results.



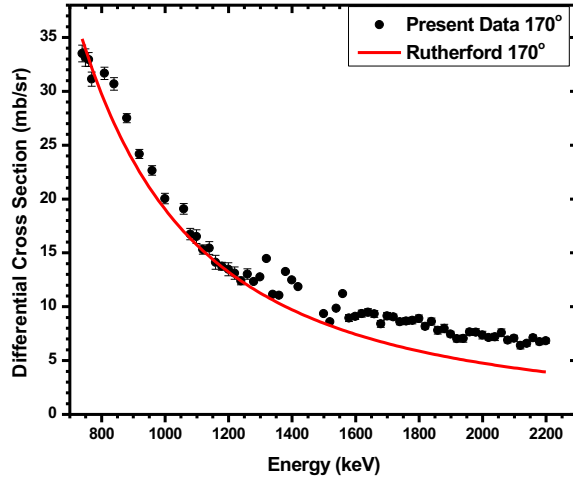


Fig. 4. (a)-(e) Differential cross section values (mb/sr) of the ${}^9\text{Be}(\text{d},\text{d}_0){}^9\text{Be}$ elastic scattering measured at $E_{\text{d,lab}} \sim 740\text{--}2200$ keV and for the scattering angles of 120° , 140° , 150° , 160° , and 170° , in variable steps, along with data from literature. The total statistical uncertainties are included in the graphs; the uncertainties are not visible in the horizontal axis due to the selected scale

CONCLUSIONS

The differential cross sections of the elastic scattering of deuterons on ${}^9\text{Be}$ were measured at five backscattering angles, namely at 120° , 140° , 150° , 160° and 170° and in the energy range $E_{\text{d,lab}} = 0.74\text{--}2.2$ MeV. The results of this work overall revealed good agreement with the existing data in literature and small deviations from the Rutherford formula at low deuteron beam energies and higher deviations at high energies. The results will soon be available to the scientific community via IBANDL (<http://www-nds.iaea.org/ibandl/>).

ACKNOWLEDGEMENT

This work has been supported by the Greek Scholarship Foundation and has been funded by the "Doctoral Research Financial Support" Act from resources of the OP "Development of Human Resources, Education and Lifelong Learning" 2014-2020, which is co-funded by the European Social Fund-ESF and the Greek Government.

References

- [1] N. Patronis et al., Nucl. Instr. Meth. Phys. Res. B 337, 97 (2014)
- [2] Ntemou et al., Nucl. Instr. Meth. Phys. Res. B in press (2018)
- [3] C. A. Kalfas at al, Nucl. Instr. Meth. Phys. Res. A 830, 265 (2016)
- [4] K. Preketes-Sigalas et al., Nucl. Instr. Meth. B 414, 99 (2018)
- [5] M. Mayer, AIP Conf. Proc. 475, 541 (1999)
- [6] G. Konac et al., Nucl. Instr. Meth. Phys. Res. B 136, 159 (1998)
- [7] G. Konac et al., Nucl. Instr. Meth. Phys. Res. B 146, 106 (1998)

- [8] Z. Liu et al., Nucl. Instr. Meth. Phys. Res. B 93, 404 (1994)
- [9] S. Krat et al., Nucl. Instr. Meth. B 358, 72 (2015)
- [10] F. Machali et al., Atomkernenergie, 13, 29 (1968)
- [11] J.M. Lombaard et al., Jour. Zeitschrift fuer Physik, 249, 349 (1972)
- [12] J.H. Renken, Phys. Rev. 132, 2627 (1963)